Soft Matter

Accepted Manuscript

ROYAL SOCIETY OF CHEMISTRY

www.rsc.org/softmatter

Optical Coherence Tomography Velocimetry of Colloidal Suspensions

A.V. Malm[1,2], A.W. Harrison[1,2,3#], and T.A. Waigh[1,2*]

[1]*School of Physics and Astronomy, University of Manchester, Oxford Rd, Manchester, M13 9PL, UK.*

[2]*Photon Science Institute, University of Manchester, Oxford Rd, Manchester, M13 9PL, UK.*

[3]*Faculty of Life Science, University of Manchester, Oxford Rd, Manchester, M13 9PL, UK*

**e-mail address: t.a.waigh@manchester.ac.uk*

[#]Now located at: *Pines Lab, Wellcome Trust/Cancer Research UK Gurdon Institute, University of Cambridge, Tennis Court Road, Cambridge CB2 1QN, UK*

Optical coherence tomography velocimetry combined with a rheometer and optical modulation techniques provides increased sensitivity to the low shear rate motion of complex fluid systems. Optical modulation coupled with a new interferometer design yields improved signal to noise ratios and is demonstrated with optically opaque colloidal suspensions. Thus the measureable range of shear velocities with complex fluids can be as low as ~40 μms^{-1}, more than an order of magnitude improvement on the previous lower limit of ~700 μms^{-1}. Furthermore the apparatus demonstrates improved sensitivity to the measurement of velocity. The instrument was used to study two hard sphere colloidal systems, sterically stabilized PVP spheres of 1μm radius and polystyrene spheres of 600 nm radius, which display shear banding behavior due to shear induced concentration gradients. OCT velocimetry also allows the velocity fluctuations of the system to be quantified as a function of the distance across the rheometer gap to help classify underlying unsteady or turbulent phenomena.

KEYWORDS: VELOCIMETRY, SHEAR BANDING, COLLOIDS, RHEOLOGY, OCT.

I. INTRODUCTION

Optical coherence tomography (OCT) velocimetry combined with a rheometer has been previously demonstrated as a powerful tool for studying flow in complex fluids [1] [2] as it provides high resolution measurements (9 μm thick slices), has probe volumes of 3.4 pl, can explore opaque fluids over a wide range of time scales and has a relatively high sample penetration depth of up to ~2 mm when compared with other optical velocimetry techniques [3] [4] such as DLS [5] and PIV [6].

The measurement of velocity profiles for a sheared system allows greater insight than that allowed by conventional bulk rheology as phenomena such as wall slip and shear banding can be directly identified. We used the OCT apparatus to probe the rheology and inter particle dynamics of the glass transition of hard-sphere colloids [7] [8] and specifically the shear banding behavior of sheared colloidal glasses [9]. The equipment was able to measure much thicker samples than in previous confocal microscopy experiments, over a wider range of time scales than comparable particle tracking experiments (OCT can probe 4 μs-1000 s dynamics) and was also able to quantify the amplitude of the velocity fluctuations.

II. IMPROVED INSTRUMENTATION

A limitation of initial embodiments of OCT velocimetry techniques was the inability to measure low shear velocities accurately due to the poor signal to noise ratio (SNR) created by the dominating effect of reciprocal frequency noise, 1/*f*, associated with standard photon-detectors at low frequencies [10]. This issue has been remedied in our current design using an Electro-optical modulator (EOM) which consists of an optically active crystal, the refractive index of which is sensitive to the electric field strength applied to it. The EOM was modulated at high frequencies of 40 kHz.

In order to incorporate the EOM into the velocimeter, a Mach-Zender interferometer was constructed (**Figure 1**), as opposed to the previous design that used a Michelson interferometer. Mach-Zender interferometers are known to yield better SNR than Michelson interferometers in OCT experiments [11].

Driving the EOM with a sinusoidal high voltage results in a periodic phase shift in the beam of the reference arm of the interferometer, which in turn generates sideband peaks in the measured power spectrum density (PSD). The equation for the measured optical power as a function of time ($P(t)$) is described by [12],

$$\boldsymbol{P(t) = P_0[1 + \cos(\omega t) + m\cos\{(\Omega \pm \omega)t\}]}, \quad (1)$$

where ω is the Doppler frequency of the fluid due to its motion, Ω is the modulation frequency of the EOM (40 kHz), m describes the degree of interference and P_0 is the average optical power.

The intensity signal from the interferometer was read into a computer, sampling at >250 kHz, and the PSD calculated using LabView. The planar reference mirror was mounted on a linear translator, and the signal from the interferometer was recorded for ~1 s for each mirror position, relating to different depths within the sample.

Whilst Fourier Domain-OCT is now preferentially used in medical imaging, a Time Domain-OCT system is currently used since it is known to be more robust and

sensitive to low SNR's than Spectral/Fourier Domain-OCT Systems [13].

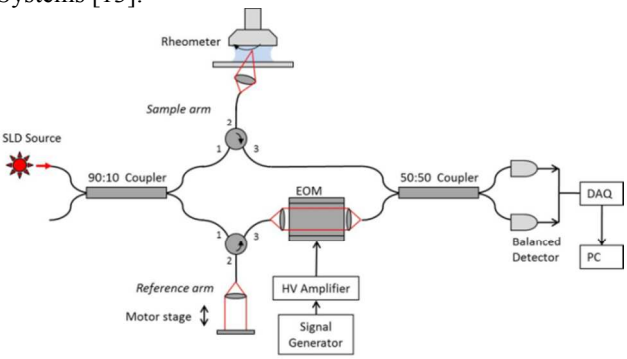

Figure 1: Schematic OCT velocimeter based around a Mach-Zender interferometer. The infrared light source (a super luminescent diode, SLD) has a wavelength of 1.3 μm and a longitudinal coherence length of 9 μm. A 90:10 coupler was used so that the majority of the light is incident on the sample in the rheometer, in order to balance the interfering intensities in the second 50:50 coupler. Circulators are used such that all the light is directed towards the detector and no light is able to reenter the source which would otherwise lead to instability in the output of the SLD.

Doppler frequencies were calculated from a Gaussian fit of the measured PSD. Demodulation of the signal is also possible, allowing the original signal to be recovered.

The shear velocity ($\boldsymbol{v}$) of the sample was calculated using,

$$\boldsymbol{v} = \frac{\boldsymbol{\lambda\omega}}{\boldsymbol{2\sin\theta}}, \quad (2)$$

where λ is the wavelength of the light source and θ is the angle between the fiber probing the sample and the shear gradient direction, which is 13° in the current setup [1].

The use of balanced heterodyne detection in the present design (**Figure 1**) has also significantly improved the SNR by allowing common mode noise to be suppressed [10].

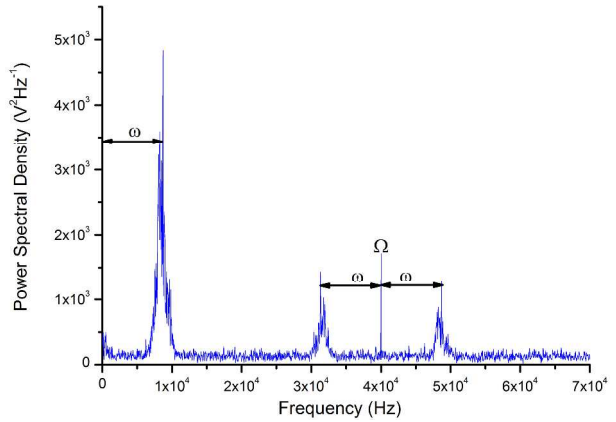

Figure 2: Example of modulated Doppler peaks (modulation frequency of 40 kHz) measured on the balanced detector as predicted by **Equation 1,** where the peak width is associated with fluctuations in the flow velocity of the sample.

The modulated sideband peaks have a comparatively lower height than the un-modulated peak, **Figure 2**, as the Noise Equivalent Bandwidth increases with frequency, however the background noise at higher frequencies is significantly lower, and the modulation peak is well defined, meaning the modulated peaks are better resolved than those obscured by the $1/f$ detector noise. The improvements in SNR at different measured shear velocities are shown in Figure 1 of the supplementary material.

The lowest measurable shear velocity with the new design is ~40 μms^{-1} for a material with a high density of scatterers or high refractive index probes, as opposed to the previous lower limit of ~700 μms^{-1} [1].

Further information can be obtained from these measurements by quantifying the standard deviation of the measured Doppler peaks, giving a measure of the scale of velocity fluctuations (δv) within the sample. This is valuable for the determination of the type of flow behavior, particularly in the categorization of unsteady flows due to non-linear instabilities such as classical turbulence or elastic (low Reynolds number) turbulence [14].

III. COLLOIDAL HARD SPHERES

Hard-sphere colloids are a useful system to demonstrate the technique of OCT velocimetry as they strongly scatter light. Furthermore they present an almost perfect hard sphere inter-particle potential, which facilitates the creation of fundamental models for their dynamics.

Two types of hard spheres were studied with different sizes and chemistries; polystyrene spheres with effective radii of 600 nm and poly-vinylphenol (PVP) spheres with effective radii of 1 μm measured using DLS. Both samples have a brush like coating of 10-15 nm long polymer chains (1.8-3k molecular weight poly-hyrdoxysteric acid) on the colloidal spheres which surround the solid core providing a quasi-hard sphere repulsion between them (steric-stabilization). Similar colloidal suspensions have been studied in depth by a group at the University of Edinburgh and shown to display shear banding [15].

It has been established that these suspensions undergo phase transitions at theoretically predicted volume fractions, ϕ, for hard spheres with notable transitions from a fluid to a glass at ϕ_g = 0.58 and a random close packed sediment at ϕ_{rcp} = 0.64 [16]. Such suspensions have previously been studied using particle imaging velocimetry (PIV) using a confocal microscope and were observed to exhibit shear banding for suspensions in the glassy phase, which is attributed to flow-concentration coupling [15], a novel mechanism different from the elastic turbulence phenomena seen with long polymeric chains and worm-like surfactants [2] [17] [18] [19] [20].

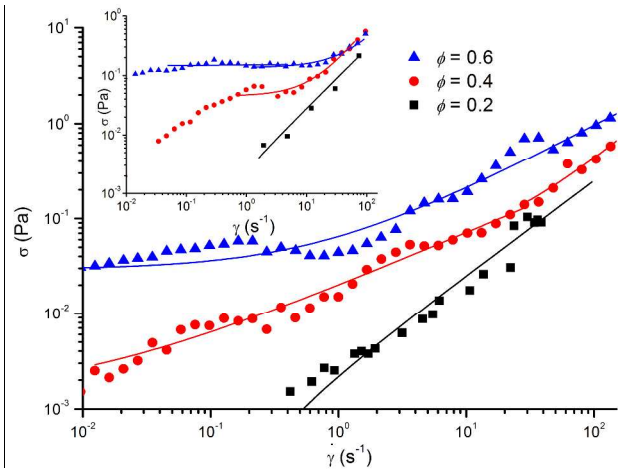

Figure 3: Measured stress (σ) as a function of shear rate for different volume fractions of PVP and polystyrene (inset[1]) colloid suspensions, displaying Herschel-Buckley type behavior (fits shown on the figure) for $\phi = 0.4$ and $\phi = 0.6$ volume fraction suspensions according to **Equation 3.** The $\phi = 0.2$ suspensions show linear behavior.

The spheres were suspended in water, with volume fractions of 0.2, 0.4 and 0.6. Although refractive index matching is a common practice in PIV, this is not necessary in OCT.

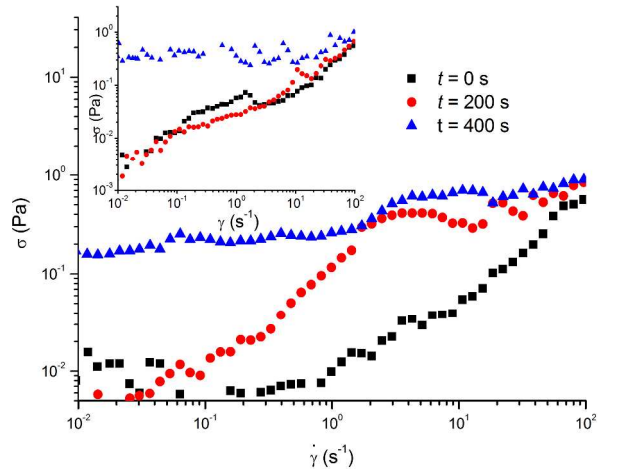

Figure 4: Stress as a function of shear rate for a $\phi = 0.6$ suspension of thixotropic PVP and polystyrene (inset) colloids over time. The legend gives the time elapsed after loading the sample when the shear ramp experiment began.

The concentrated colloidal samples provide a challenge for velocimetry as they are optically opaque and standard PIV cannot be used for thick samples (<2 mm). OCT velocimetry however can probe such opaque materials and can also measure velocity profiles for macroscopic sample thicknesses larger than PIV bright field microscopy and confocal sample limits. Additionally it is relatively easy to extract the magnitude of the velocity fluctuations for pico-liter volumes of specimens; as such OCT velocimetry can provide complementary and sometimes superior characterization of complex fluid dynamics.

IV. BULK RHEOLOGY

Controlled shear rate measurements performed using a rheometer for aqueous colloidal suspensions show that there is generally shear thickening behavior above shear rates ($\dot{\gamma}$) of greater than 1 s^{-1} for the $\phi = 0.4$ and 0.6 suspensions, **Figure 3.** The $\phi = 0.6$ solutions demonstrate Herschel-Buckley type behavior, where at low shear rates, the material acts like a solid, with a certain yield stress, σ_y, needed to make the sample flow, where the shear stress (σ) is described by Equation 3,

$$\boldsymbol{\sigma = \sigma_y + k\dot{\gamma}^n}, \quad (3)$$

where k and n are constants for the consistency and flow index of the material respectively.

The $\phi = 0.4$ suspensions appear to show Herschel-Buckley behavior, however at much lower shear rates, the sample is still a fluid[2]. This shear thickening behavior can allow the suspension to be driven into a localized glass transition when the material is under shear due to jamming and concentration fluctuations [21] [22] [23].

The plateau and the apparent wobble in the flow curves is typical of systems where instabilities associated with shear banding take place [24]. This can also be attributed to non-uniform stresses within the sample material given that a parallel plate geometry is used and the shear stress is measured over a wide range of shear rates. Additional measurements demonstrate that these suspensions are also thixotropic, with stress curves evolving over time with an increase in apparent yield stress, **Figure 4**. Although this could be attributed to sedimentation, and therefore a decrease in volume fraction over time, this would result in a decrease in yield stress being observed and is therefore not the cause of this time dependency.

V.VELOCIMETRY

Prior to each experiment, the velocimeter was first calibrated using a dilute suspension of silica spheres (r=0.27μm, 1% w/w), which is known to act as a Newtonian fluid. The measured velocity profiles were rescaled by the rheometer gap, z_g (300μm), and the upper plate velocity, v_g, in order to allow comparison between samples/experiments.

[1] Large versions of the inset figures are included in the supplementary material.

[2] Flow curves showing behaviour at lower shear rates are included in the supplementary material.

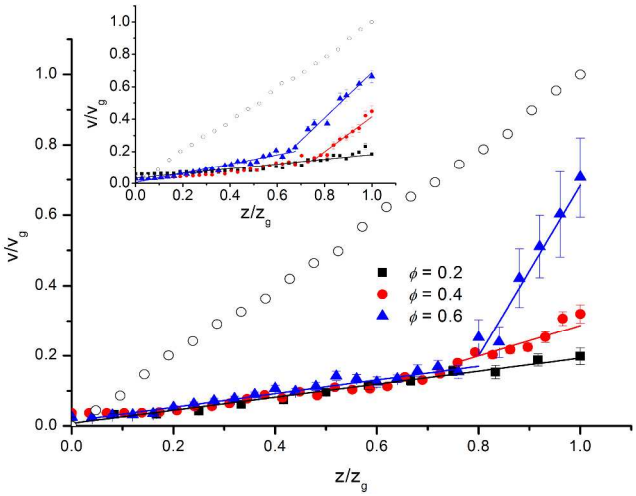

Figure 5: Rescaled shear velocity (v/v_g) as a function of rescaled depth across the rheometer gap (z/z_g) for three different volume fraction suspensions of PVP colloids ($\dot{\gamma} = 100$ s^{-1}). The inset shows the results for polystyrene colloids at the same three volume fractions. The open circles show the profile for a dilute suspenion of silica tracer paticles used to calibrate the experiment. The error bars signify the apparent velocity fluctuations at each depth within the sample.

A plate-plate rheometer geometry was used with a stationary glass lower plate and a Perspex upper plate under controlled shear, similar behavior was seen when a Perspex lower plate is also used (data not shown).

In comparison with the linear profile of a Newtonian fluid, **Figure 5** shows that all of the colloidal suspensions display significant wall slip at the upper plate. Whilst the $\phi = 0.2$ suspensions display linear profiles, the higher concentrations show an increasing departure from linearity, with the extent of apparent banding increasing with shear rate, **Figure 6**.

The fits shown in the velocity profiles in **Figures 5-7** are linear profiles which are later used to calculate the shear rate of each band, **Figure 10**.

The samples demonstrated significant thixotropy, and velocity profiles were observed to evolve over time. Those shown in **Figure 5 and 6** were all recorded directly after the sample was loaded into the rheometer and **Figure 7** shows the change in velocity over time, with profiles recorded for increasing periods of prior shearing.

Whilst sedimentation could be taking place whilst the sample is sheared, the evolution of the velocity profiles suggest that this is not the cause of the observed banding, as the amount of sample in the lower band does not increase with time, and the $\phi = 0.2$ suspensions show no banding at all.

In the velocity profiles discussed, the velocity fluctuations appear to increase at the upper plate of the rheometer. In order to verify that this is not a simple scaling with increased velocity, the reduced velocity fluctuations, $\delta v/v$, are plotted as function of distance across the rheometer gap, **Figure 8**.

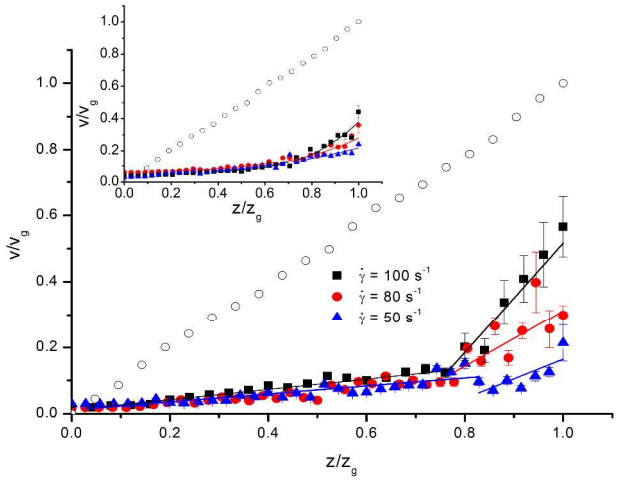

Figure 6: Scaled shear velocity (v/v_g) as a function of normalized distance across the rheometer gap (z/z_g) for dense suspensions of PVP hard spheres ($\phi = 0.6$), showing shear banding and slipping at the upper plate ($z/z_g = 1$). The error bars signify the apparent velocity fluctuations at each depth within the sample. The inset shows similar data for polystyrene suspensions

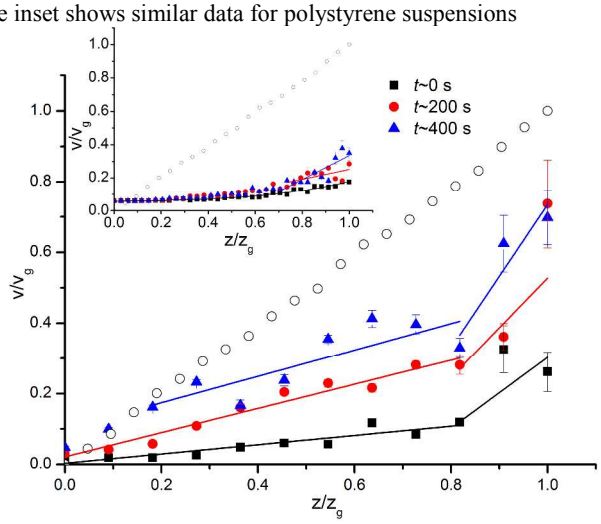

Figure 7: Shear velocity as a function of depth across the rheometer gap for a $\phi = 0.6$ PVP and polystyrene (inset) suspensions with steady shear rate of 50 s^{-1} recorded at different intervals after sample loading. Thixotropy of the samples is evident in the velocity profiles.

As expected from hydrodynamic theory, the velocity fluctuations approach zero close to the stationary lower plate [25]. Away from the lower plate, velocity fluctuations increase but remain approximately constant across the bulk of the fluid. In the case of the higher volume fraction suspensions, there is an increase in the velocity fluctuations at the same corresponding depth where the velocity profiles also became non-linear, associated with the change in behavior of the upper shear band. Thus the high velocity regions of the flow are relatively more unstable than the low velocity regions when banding occurs i.e. broadly there is an upper band of more

turbulent, highly fluctuating motion and a lower band of less turbulent motion with lower fluctuations.

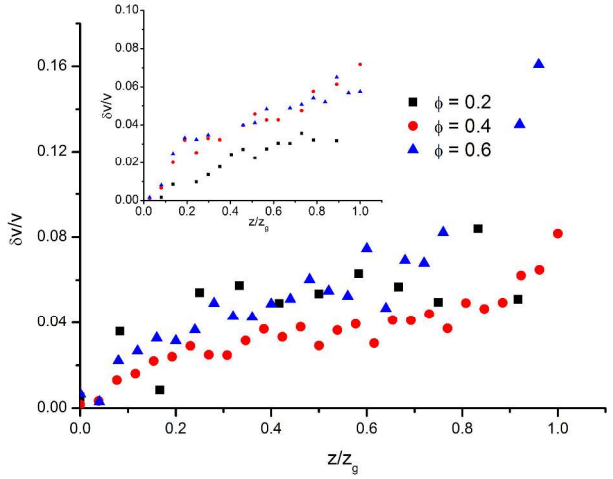

Figure 8: Reduced velocity fluctuations ($\delta v/v$) as a function of distance (z/z_g) across the rheometer gap for dense PVP suspensions (ϕ = 0.6). The inset shows similar velocity fluctuation profiles for polystyrene suspensions.

The velocity profiles in **Figures 5-7** all show considerable slipping at the upper plate. In order to remove this slipping, velocity profiles were measured with rheometer plates that had been spin coated with a layer of colloids. **Figure 9** shows a comparison of velocity profiles with and without this coating process, showing that this does indeed reduce slipping but does not change the functional form of the profile and thereby confirms that the non-linearity observed for the uncoated plates are as a result of shear banding.

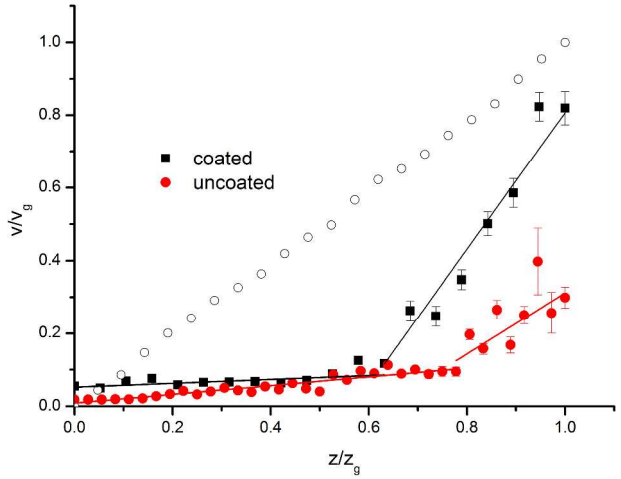

Figure 9: Scaled shear velocity (v/v_g) as a function of scaled distance across the rheometer gap (z/z_g) for dense PVP suspensions (ϕ = 0.6) with a shear rate of 80 s^{-1}, both with coated and uncoated rheometer plates. The uncoated plate showing greater wall slip than the coated plate, as expected.

Models for shear banding materials often refer to a lever rule, **Equation 4**, where the shear rate ($\dot{\gamma}$) at the upper plate is related to the shear rate and volume of sample (φ) in the lower and higher bands.

$$\dot{\gamma} = \varphi_l \dot{\gamma}_l + \varphi_h \dot{\gamma}_h \quad (4)$$

By definition, $\varphi_h = 1 - \varphi_l$, and the value of φ_l can be read from the velocity profiles as the depth within the sample where an inflection occurs, and the two shear rates are calculated as the gradient of each band.

A comparison between the measured upper plate shear rate and the value calculated from **Equation 4** gives an approximate linear relationship, **Figure 10**.

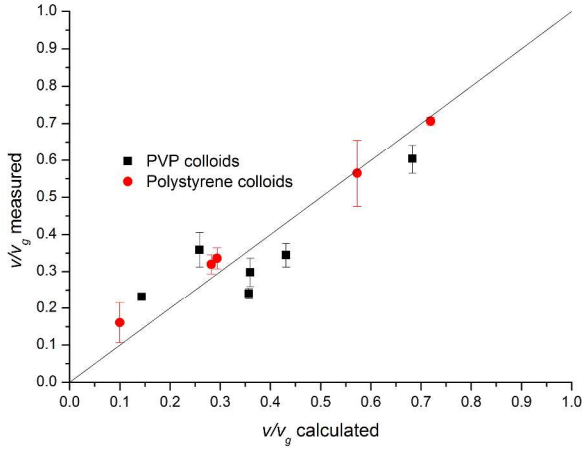

Figure 10: Measured velocity at the upper plate as a function of calculated velocity calculated from Equation 4 for the two types of colloids.

Future work will attempt to quantify the fluctuations of the shear banded states in more detail e.g. currently we only measure velocity fluctuations in the flow direction, whereas three dimensional measurements are technically feasible to quantify flow velocity and fluctuations in the velocity, shear gradient and vorticity directions independently.

Possible extensions to the OCT technique include using phase measurements of the interferometer signal to further improve sensitivity to low velocity measurements [26].

VI. CONCLUSIONS

Our improved OCT velocimetry instrumentation is demonstrated to have greater sensitivity to low shear rates and allows improved quantification of velocity fluctuations in complex fluids. Specifically with colloidal glasses, larger sample thicknesses can be probed than with previous methods, over a wider range of time scales. The OCT measurements indicate a dynamic phase separation in the colloidal glasses between a high velocity, highly fluctuating band and a low velocity band with lower velocity fluctuations. Shear banding behavior is observed for dense colloidal suspensions of $\phi \geq 0.4$, both above and below the glass phase volume fraction.

Although wall slip is observed, it can be seen that banding still occurs once wall slip has been removed by coating the rheometer plates in a layer of colloids.

ACKNOWLEDGEMENTS

The authors would like to thank *Dr Andrew Schofield* from the University of Edinburgh, for providing the colloidal samples, *Malvern Instruments* for the gift of a fluids rheometer and *Gian Fulgoni* for financial support of Alex Malm.

The OCT velocimetry technique is patented [27], but for information on how to build a non-commercial OCT velocimeter please contact *Alex Malm* directly, alex.malm@manchester.ac.uk.

REFERENCES

[1] M. Harvey and T. Waigh, "Optical coherence tomography velocimetry in controlled shear flow.," *Phys Rev E,,* no. 83, p. 31502, 2011.

[2] S. Jaradat, M. Harvey and T. Waigh, "Shear banding in polyacrylamide solutions revealed via optical coherence tomography velocimetry," *Soft Matter,* no. 8, p. 11677, 2012.

[3] G. Fuller, Optical rheometry of complex fluids, OUP, 1995.

[4] S. Manneville, "Recent experimental probes of shear banding," *Rheol. Acta,* no. 47, p. 301, 2008.

[5] S. E. Phan, W. B. Russel and e. al, "Phase transition, equation of state, and limiting shear viscosities of hard shere dispersions," *Phy Rev E,* vol. 64, no. 6, pp. 6633-6645, 1996.

[6] L. Isa, R. Besseling, A. B. Schofield and W. C. Poon, "Confocal imaging of dense colloidal flows," *Advances in Polymer Science,* vol. 236, pp. 163-202, 2010.

[7] G. Hunter and E. Weeks, "The physics of the colloidal glass transition," *Reports on progress in physics,* vol. 75, p. 066501, 2012.

[8] D. Denisov, M. Dang, B. Struth, G. Wegdam and P. Schall, "Resolving structural modifications of," *Science Reports,* vol. 3, no. 1631, 2013.

[9] J. Mewis and J. Wagner, Colloidal Suspension Rheology, CUP, 2011.

[10] H. Haus, Electromagnetic noise and quantum optical measurements, Springer, 2000.

[11] A. Rollins and A. Izatt, "Optimal interferometer designs for optical coherence tomography," *Optics Letters, 24,,* vol. 24, no. 21, pp. 1484-1486, 1999.

[12] R. Belansky and K. Wanser, "Laser doppler velocimetry using a bulk optic Michelson interferometer," *American Journal of Physics,* no. 63, pp. 1014-1019, 1993.

[13] M. Szkulmowski, A. Szkulmowska, T. Bajraszewski, A. Kowalczyk and M. Wojtkowsk, "Flow velocity estimation using joint Spectral and Time domain Optical Coherence Tomography," *Optics Express,* vol. 16, no. 9, pp. 6008-6025, 2008.

[14] V. Steinberg and A. Groisman, "Elastic turbulence in a polymer solution flow," *Nature,* no. 405, pp. 53-55, 2000.

[15] R. Besseling, L. Isa, W. Poon, P. Ballesta, G. Petekidis and M. Cates, "Shear banding and flow-concentration coupling in colloidal glasses," *PRL,* no. 105, 2010.

[16] P. Pusey and W. Megen, "Phase behaviour of concentrated suspensions of nearly hard colloidal spheres," *Nature,* no. 320, pp. 340-342, 1986.

[17] J. Beaumont, "Turbulent flows in highly elastic worm-like micelles," *Soft Matter,* vol. 9, no. 3, pp. 735-749, 2013.

[18] I. Kunita, "Shear banding in an F-actin solution," *PRL,* vol. 24, no. 109, p. 248303, 2012.

[19] L. Walker, "Rheology and structure of worm-like micelles," vol. 6, pp. 451-456, 2001.

[20] S. Wang, S. Ravindranath and P. E. Boukany, "Homogeneous Shear, Wall Slip, and Shear Banding of Entangled Polymeric Liquids in Simple-Shear Rheometry: A Roadmap of Nonlinear Rheology," *Macromolecules,* vol. 44, no. 2, pp. 183-190, 2011.

[21] A. W. H. L. G. Wilson, A. Schofield, J. Arlt and W. Poon, "Passive and active microrheology of hard-sphere colloids," *J. Phys Chem B,* vol. 113, no. 12, pp. 3806-3812, 2009.

[22] P. Ballesta, A. Duri and L. Cipelletti, "Unexpected drop of dynamical heterogeneities in colloidal suspensions approaching the jamming transition," *Nature Physics,* vol. 4, pp. 550-554, 2008.

[23] A. Liu and S. Nagel, Jamming and Rheology, Tayloe and Francis, 2001.

[24] P. Schall and M. Hecke, "Shear banding in matter with granularity," *Annu. Rev. Fluid Mech.,* vol. 42, pp. 67-88, 2010.

[25] S. Pope, Turbulent flows, CUP, 2000.

[26] Y. Zhao, Z. Chen, C. Saxer, S. Xiang, J. F. d. Boer and J. S. Nelson, "Phase-resolved optical coherence tomography and optical Doppler tomography for imaging blood flow in human skin with fast scanning speed and high velocity sensitivity," *OPTICS LETTERS,* vol. 25, no. 2, pp. 114-116, 2000.

[27] M. Harvey and T. Waigh, "OCT Rheometer Patent". Patent 1013945, 2010.